Dyes and Pigments 82 (2009) 95–101

Contents lists available at ScienceDirect

Dyes and Pigments

journal homepage: www.elsevier.com/locate/dyepig

Anyles of 4-benzoylpyridine – Crystal structure and spectroscopic properties

T. Kolev [a,*], T. Tsanev [b], S. Kotov [c], H. Mayer-Figge [a], M. Spiteller [a], W.S. Sheldrick [a], B. Koleva [a]

[a] Lehrstuhl für Analytische Chemie, Ruhr-Universität Bochum, Universitätsstraße 150, 44780 Bochum, Germany
[b] Institut für Umweltforschung, Universität Dortmund, Otto-Hahn-Strasse 6, 44221 Dortmund, Germany
[c] Burgas University, Faculty of Chemistry, 1, J. Bouchier, Blvd., 1164 Burgas, Bulgaria

ARTICLE INFO

Article history:
Received 6 November 2008
Received in revised form
27 November 2008
Accepted 29 November 2008
Available online 7 December 2008

Keywords:
Anyles
Crystal
structure
Solid-state linear polarized IR-spectroscopy
UV-, Quantum chemical calculations
^{1}H and ^{13}C NMR
UV-, ESI MS, TGV and DSC

ABSTRACT

Two novel anyles of 4-benzolylpyridine, namely *N*,*N*-diethyl-*N*′-[(*Z*)-phenyl(pyridin-4-yl)methylidene]-benzene-1,4-diamine and its *N*-ethylpyridinium salt were synthesized and elucidated in detail spectroscopically, thermally and structurally, using linear polarized solid-state IR-spectroscopy, UV-spectroscopy, TGA, DSC, DTA and positive and negative ESI MS. Quantum chemical calculations were used to obtain the electronic structure, vibrational data and electronic spectra of the compounds. The crystal structure of an anyle-pyridine derivative, *N*,*N*-diethyl-*N*′-[(*Z*)-phenyl(pyridin-4-yl)methylidene]-benzene-1,4-diamine, is reported for the first time; the material crystallized in the triclinic *P*-1 space group and only one short contact of length 3.16 Å was observed between two neighbouring pyridine fragments. A bathochromic shift in λ_{max} of 170 nm resulted from *N*-anylation and a 95 nm solvatochromic shift of *N*,*N*-diethyl-*N*′-[(*Z*)-phenyl(pyridin-4-yl)methylidene]benzene-1,4-diamine were obtained depending on solvent type.

1. Introduction

Interest in pyridine salts during the past 30 years has been due to many of the derivatives possessing large second-order molecular hyperpolarizabilities. Studies of the second harmonic generation (SHG) from powders and Langmuir–Blodgett films of merocyanine dyes have attracted much attention due to their application in various areas of non-linear optics. Second-order non-linear optical properties of these materials are very sensitive to the symmetry of the structure [1–4]. It has been found that the variation of the counter ion in organic salts provides a simple and highly successful approach to create materials with larger χ values. This methodology has been also supported by the observed crystal structure and properties of DAST [1].

We now present a spectroscopic and structural elucidations of the novel compound *N*,*N*-diethyl-*N*′-[(*Z*)-phenyl(pyridin-4-yl)methylidene]benzene-1,4-diamine and its *N*-ethyl pyridinium iodide (Scheme 1) as part of our systematic study of new materials with potential NLO application [5–8]. The relationship between its structural and spectroscopic properties has been elucidated using single crystal X-ray diffraction, UV–vis and fluorescence methods, polarized linear-dichroic infrared (IR-LD) spectroscopy of oriented colloid suspensions in a nematic liquid crystal, mass spectrometry and TGV and DSC methods. To the best of our knowledge the crystal structure of *N*,*N*-diethyl-*N*′-[(*Z*)-phenyl(pyridin-4-yl)methylidene]benzene-1,4-diamine represents the first example of a structural study of a compound of the anyle class.

2. Experimental

2.1. Methods

The X-ray diffraction intensities were measured in the ω scan mode on a Siemens P4 diffractometer equipped with Mo K_α radiation ($\lambda = 0.71073$ Å, $\theta_{max} = 25°$) [9,10]. The structure was solved by direct methods and refined against F^2 [17,18]. An ORTEP plot illustrates the anion and cation structures at the 50% probability level. Relevant crystallographic structure data and refinement details are presented in Table 1, selected bond distances and angles in Table 2. The hydrogen atoms were constrained to calculated positions and refined using riding models in all cases.

Conventional and polarized IR-spectra were measured on a Thermo Nicolet OMNIC FTIR-spectrometer (4000–400 cm^{-1}, 2 cm^{-1} resolution, 200 scans) equipped with a Specac wire-grid polarizer. Non-polarized solid-state IR spectra were recorded using the KBr disk technique. The oriented samples were obtained as

* Corresponding author. Tel.: +49 0231 755 70 69.
E-mail address: t.kolev@infu.uni-dortmund.de (T. Kolev).

0143-7208/$ – see front matter © 2008 Elsevier Ltd. All rights reserved.
doi:10.1016/j.dyepig.2008.11.008

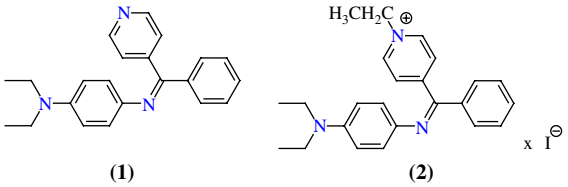

Scheme 1. Chemical diagram of *N*,*N*-diethyl-*N*′-[(*Z*)-phenyl(pyridin-4-yl)methylidene]benzene-1,4-diamine (**1**) and its *N*-ethyl pyridinium iodide (**2**).

a colloid suspension in a nematic liquid crystal ZLI 1695 [11–16]. The theoretical approach as well as the experimental technique for preparing the samples and procedures for polarized IR-spectra interpretation and the validation of this new linear-dichroic infrared (IR-LD) orientation solid-state method for accuracy and precision have been previously presented. The influence of the liquid crystal medium on peak positions and integral absorbances of the guest molecule bands, the reological model, the nature and balance of the forces in the nematic liquid crystal suspension system, and the morphology of the suspended particles have also been discussed [19–22]. The reological model is a mathematical model describing the interactions in the heterogenic system, solid particles with different sizes and morphology, liquid crystal medium and the interactions with the KBr-plates.

The positive and negative ESI mass spectra were recorded on a Fisons VG Autospec instrument employing 3-nitrobenzyl alcohol (Sigma–Aldrich) as the matrix. The method allows obtaining the weights of cations' (positive) and anions' (negative) species in the novel compounds, during the ionization processes.

Ultraviolet (UV-) spectra were recorded on Tecan Safire Absorbance/Fluorescence XFluor 4 V 4.40 spectrophotometer operating between 190 and 900 nm, using water, methanol, dichloromethane, tetrahydrofurane, acetonitrile, acetone, 2-propanol and ethyl acetale (all Uvasol, Merck products) as solvents at a concentration of 2.5×10^{-5} M in 0.921 cm quartz cells.

Quantum chemical calculations were performed with the GAUSSIAN 98 program package [23]. The output files were visualized by means of the ChemCraft program [24]. The geometries of (**1**) and (**2**) were optimized at two levels of theory: second-order Moller–Pleset perturbation theory (MP2) and density functional theory (DFT) using the 6-311++G** basis set. The DFT method employed is B3LYP, which combines Backe's three-parameter

Table 1
Crystal and refinement data for *N*,*N*-diethyl-*N*′-[(*Z*)-phenyl(pyridin-4-yl)methylidene]benzene-1,4-diamine.

Empirical formula	$C_{44}H_{46}N_6$	
Formula weight	658.87	
Temperature (K)	293(2)	
Wavelength (Å)	0.71073	
Crystal system, space group	Triclinic, *P*-1	
Unit cell dimensions	$a = 9.0240(18)$ Å	$\alpha = 98.03(3)^\circ$
	$b = 14.639(3)$ Å	$\beta = 93.91(3)^\circ$
	$c = 14.931(3)$ Å	$\gamma = 103.78(3)^\circ$
Volume (Å^3)	1886.3(7)	
Z	2	
Calculated density (mg m^{-3})	1.160	
Absorption coefficient (mm^{-1})	0.069	
F(000)	604	
Crystal size (mm)	$0.31 \times 0.25 \times 0.48$	
θ range for data collection	$2.16 \le \theta \le 25.0$	
Limiting indices	$-10 \le h \le 0$, $-16 \le k \le 17$, $-17 \le l \le 17$	
Reflections collected/unique	6607/6455, $R(\text{int}) = 0.0468$	
Absorption correction	ψ scans	
Goodness-of-fit on F^2	0.891	
Final *R* indices [$I > 2\sigma(I)$]	$R1 = 0.0824$, $wR2 = 0.1339$	
R indices (all data)	$R1 = 0.1732$, $wR2 = 0.2631$	

Table 2
Selected bond lengths [Å] and angles [°] for *N*,*N*-diethyl-*N*′-[(*Z*)-phenyl(pyridin-4-yl)methylidene]benzene-1,4-diamine from crystallographic data.

N1 C1 1.296(5)	C31 C36 1.393(5)
N1 C31 1.415(5)	C32 C33 1.389(5)
N2 C15 1.329(8)	C33 C34 1.412(5)
N2 C13 1.360(9)	C34 C35 1.395(5)
N3 C34 1.395(5)	C35 C36 1.395(5)
N3 C51 1.457(5)	C41 C42 1.541(5)
N3 C41 1.467(5)	C41 H411 0.9700
N4 C6 1.286(5)	C51 C52 1.522(6)
N4 C81 1.426(5)	C61 C62 1.385(5)
N5 C65 1.353(6)	C61 C66 1.388(6)
N5 C63 1.366(7)	C62 C63 1.408(6)
N6 C84 1.381(5)	C65 C66 1.409(6)
N6 C91 1.453(5)	C71 C72 1.400(5)
N6 C93 1.504(5)	C71 C76 1.406(5)
C1 C11 1.499(6)	C72 C73 1.380(6)
C1 C21 1.501(6)	C73 C74 1.353(6)
C6 C71 1.494(6)	C74 C75 1.359(6)
C6 C61 1.509(5)	C75 C76 1.395(5)
C11 C16 1.373(6)	C81 C82 1.393(5)
C11 C12 1.397(6)	C81 C86 1.401(5)
C12 C13 1.417(9)	C82 C83 1.385(5)
C15 C16 1.381(7)	C83 C84 1.416(5)
C21 C22 1.390(6)	C84 C85 1.393(5)
C21 C26 1.400(5)	C85 C86 1.391(5)
C23 C24 1.374(6)	C91 C92 1.513(6)
C25 C26 1.394(6), C31 C32 1.391(5)	C93 C94 1.512(6)
C1 N1 C31 122.2(4)	C33 C32 C31 122.3(4)
C15 N2 C13 119.5(8)	C32 C33 C34 121.5(4)
C34 N3 C51 120.7(4)	N3 C34 C35 121.7(4)
C34 N3 C41 120.4(4)	N3 C34 C33 122.1(4)
C51 N3 C41 117.5(4)	C35 C34 C33 116.2(4)
C6 N4 C81 125.2(4)	C36 C35 C34 121.5(4)
C65 N5 C63 117.4(5)	C31 C36 C35 122.3(4)
C84 N6 C91 122.7(4)	N3 C41 C42 114.2(4)
C84 N6 C93 121.0(4)	N3 C51 C52 115.9(4)
C91 N6 C93 115.9(4)	C62 C61 C66 117.8(4)
N1 C1 C11 124.7(4)	C62 C61 C6 122.1(5)
N1 C1 C21 116.8(4)	C66 C61 C6 120.1(4)
C11 C1 C21 118.3(4)	C61 C62 C63 119.9(5)
N4 C6 C71 117.9(4)	N5 C63 C62 122.4(5)
N4 C6 C61 125.4(4)	N5 C65 C66 122.3(5)
C71 C6 C61 116.7(4)	C61 C66 C65 120.1(5)
C16 C11 C12 117.2(5)	C72 C71 C76 117.3(4)
C16 C11 C1 121.2(5)	C72 C71 C6 123.2(4)
C12 C11 C1 121.6(5)	C76 C71 C6 119.3(4)
C11 C12 C13 120.2(7)	C73 C72 C71 121.0(5)
C11 C12 H12 119.9	C74 C73 C72 121.1(5)
C13 C12 H12 119.9	C73 C74 C75 119.5(5)
N2 C13 C12 119.9(8)	C74 C75 C76 121.7(5)
N2 C15 C16 122.3(7)	C75 C76 C71 119.4(4)
C11 C16 C15 120.9(6)	C82 C81 C86 116.9(4)
C22 C21 C26 118.4(5)	C82 C81 N4 126.1(4)
C22 C21 C1 120.1(4)	C86 C81 N4 116.7(4)
C26 C21 C1 121.5(4)	C83 C82 C81 122.1(4)
C21 C22 C23 120.1(5)	C82 C83 C84 120.8(4)
C24 C23 C22 121.4(5)	N6 C84 C85 121.7(4)
C25 C24 C23 119.0(5)	N6 C84 C83 121.2(4)
C24 C25 C26 120.9(5)	C85 C84 C83 117.1(4)
C25 C26 C21 120.2(5)	C86 C85 C84 121.4(4)
C32 C31 C36 116.2(4)	C85 C86 C81 121.6(4)
C32 C31 N1 125.7(4)	N6 C91 C92 114.5(4)
C36 C31 N1 117.9(4)	N6 C93 C94 110.7(4)

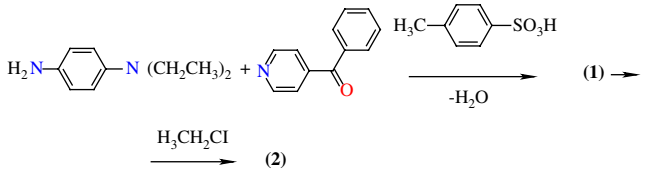

Scheme 2. Reaction scheme for obtaining of (**1**) and (**2**).

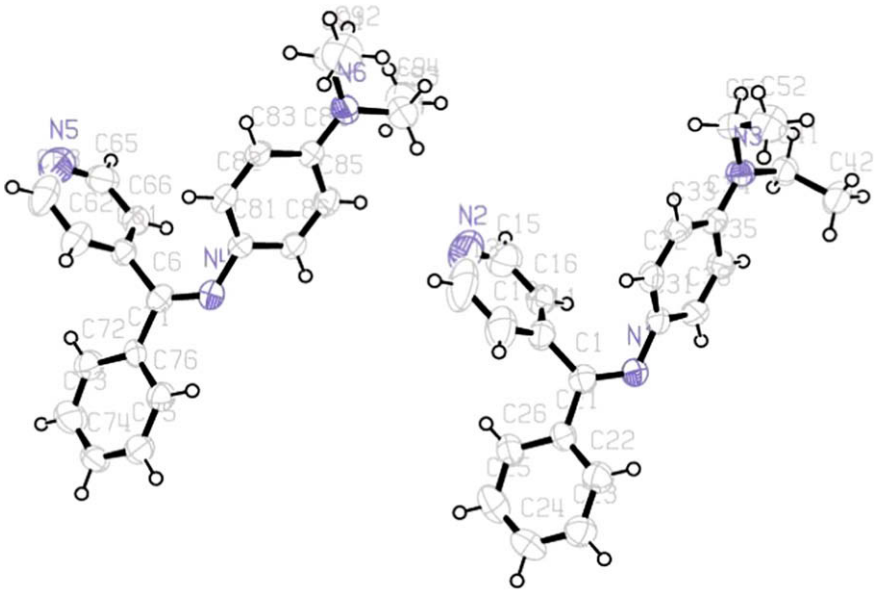

Fig. 1. The molecular structure of *N*,*N*-diethyl-*N*′-[(*Z*)-phenyl(pyridin-4-yl)methylidene]benzene-1,4-diamine, showing the atom-labeling scheme. Displacement ellipsoids are drawn at the 50% probability level.

non-local exchange function with the correlation function of Lee, Yang and Parr. Molecular geometries of the studied species were fully optimized by the force gradient method using Bernys' algorithm. For every structure the stationary points found on the molecule potential energy hypersurfaces were characterized using standard analytical harmonic vibrational analysis. The absence of imaginary frequencies, as well as of negative eigenvalues of the second-derivative matrix, confirmed that the stationary points correspond to minima of the potential energy hypersurfaces. The calculations of vibrational frequencies and infrared intensities were checked to establish which kind of performed calculations agree best with the experimental data. In our cases the DFT method provides more accurate vibrational data, as far as the calculated standard deviations of, respectively, 12 cm^{-1} (B3LYP) and 17 cm^{-1} (MP2) corresponding to groups which do not participate in intra- or intermolecular interactions are concerned. So, the B3LYP/6-311++G** data are presented for the above discussed modes, where a modification of the results using the empirical scaling factor 0.9614 was made to achieve better correspondence between the experimental and theoretical values. The UV-spectra of (**1**) in the gas phase and in ethanol solution were obtained by CIS/6-311++G** and TDDFT calculations.

The thermal analyses were performed in the 300–500 K region on a Differential Scanning Calorimeter Perkin–Elmer DSC-7, and a Differential Thermal Analyzer DTA/TG (Seiko Instrument, model TG/DTA 300). The experiments were carried out with a scanning rate of 10 K/min under an argon atmosphere.

The elemental analysis was carried out according to the standard procedures for C and H (as CO_2, and H_2O) and N (by the Dumas method).

2.2. Synthesis

N,*N*-Diethyl-*N*′-[(*Z*)-phenyl(pyridin-4-yl)methylidene]benzene-1,4-diamine (**1**) was synthesized as follows: a solution of 0.2 mol 4-benzolpyridine dissolved in 40 ml toluene was mixed with *N*, *N*-diethyl-4-phenylendiamine and 0.04 g *p*-toluene acid was added. The resulting solution was heated for 2 h at 140 °C

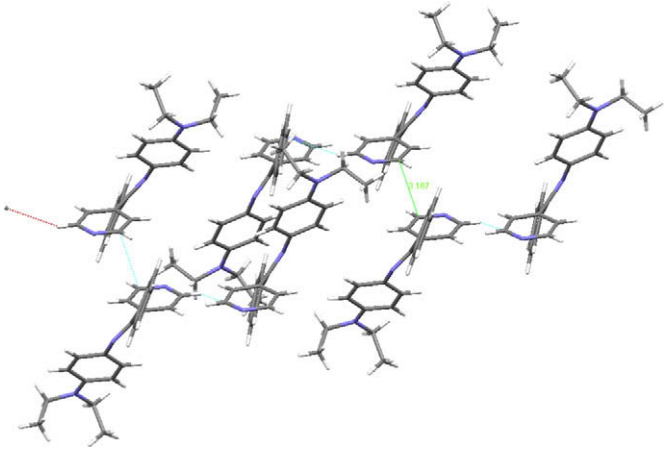

Fig. 2. Linkage of the molecules of (**1**).

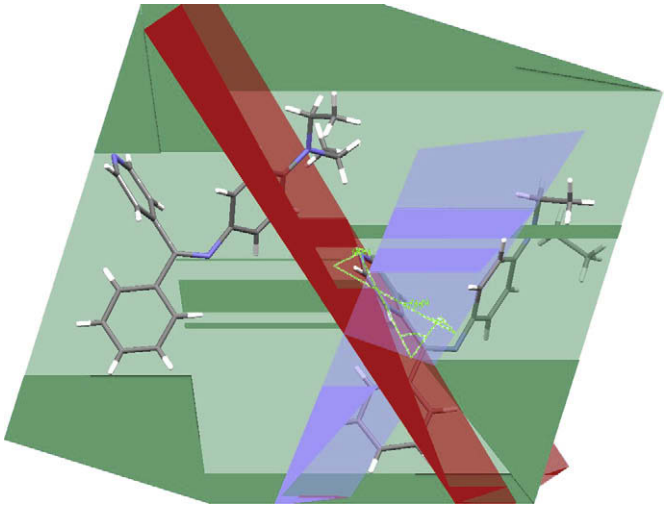

Fig. 3. Mutual orientation of the aromatic fragments in the molecule of (**1**).

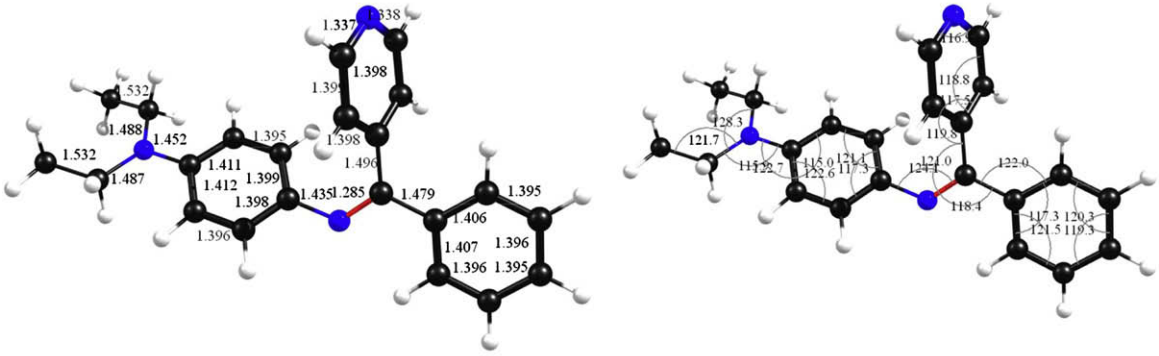

(1)

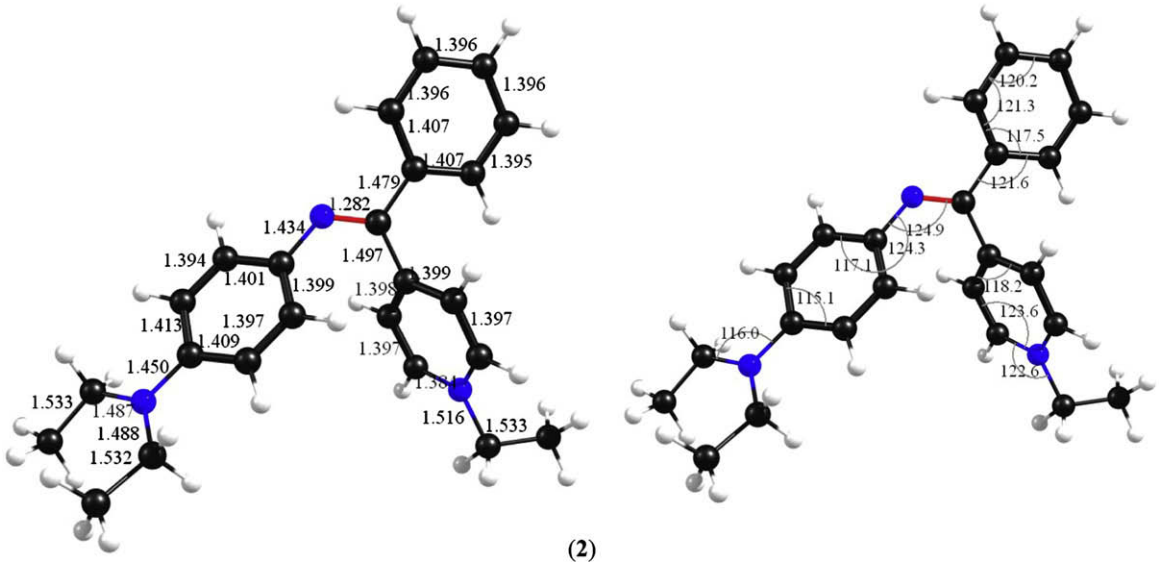

(2)

Scheme 3. Most stable conformers of (**1**) and (**2**) with corresponding geometry parameters, *i.e.* bond lengths [Å] and angles [°].

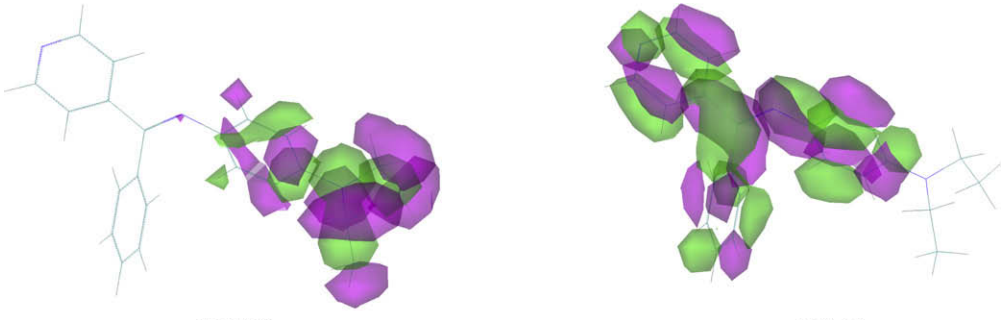

(1)

(2)

Scheme 4. Molecular orbital surface of the HOMO and LUMO for the ground state of (**1**) and (**2**).

(Scheme 2) and after cooling the reaction product was recrystallized from ethanol over a period of 7 d. Yield 78%. The corresponding *N*-ethylpyridinium iodide (**2**) was obtained by mixing a toluene solution of (**1**) with iodoethane at equimolar amounts, under continuous stirring and heating at 70 °C for 3 h. Compound (**2**) was isolated by extraction with water. Yield 90% (Scheme 2). Found (**1**): C, 80.20; H, 7.04; N, 21.73; [$C_{22}H_{23}N_3$] calcd. (**1**): C, 80.21; H, 7.04; N, 21.75%. Found (**2**): C, 59.40; H, 5.81; N, 8.67; [$C_{22}H_{28}N_3I$] calcd. (**2**): C, 59.39; H, 5.81; N, 8.66%. The most intensive signals in the positive ESI mass spectra of (**1**) and (**2**) are those at *m*/*z* 330.40 and 358.77, corresponding to the singly charged cations $[C_{22}H_{24}N_3]^+$ and $[C_{24}H_{28}N_3]^+$, with molecular weights of 350.45 and 358.51, respectively. The TGV and DSC data in temperature range of 300–500 K show an absence of solvate molecules in both compounds.

3. Results and discussion

3.1. Crystal structure of N,N-diethyl-N′-[(Z)-phenyl(pyridin-4-yl)methylidene]benzene-1,4-diamine (1)

Compound (**1**) crystallizes in the triclinic space group *P*-1 (Fig. 1) and its unit cell contains two pairs of non-equivalent molecules, differing in the values of the dihedral angles of the $(CH_3)CH_2NCH_2CH_3$ chain of 100.9(0)° and 96.0(7)°, respectively (Fig. 1). Only one short contact between two neighbouring pyridine fragments is found with a length of 3.16(7) Å (Fig. 2). The planes of the aromatic fragments are oriented at mutual angles of 57.8(5)°, 71.6(9)° and 66.0(4)°, respectively (Fig. 3), thus ruling out any type of π conjugation.

3.2. Theoretical calculations

The conformational analysis was performed by variation of the dihedral angle values. Scheme 3 depicts the most stable conformers of (**1**) and its *N*-ethylpyridinium derivative (Scheme 1) corresponding to *E* values of 0.1 kJ/mol (**1**) and 0.0 kJ/mol (**2**). The geometrical parameters (*i.e.* bond lengths and angles) are depicted in Scheme 3, thus indicating an excellent agreement between the theoretical values and the crystallographic data for (**1**) (compare Scheme 3 and Table 2). Differences of less then 0.0341 Å and 2.4(1)° are obtained. The theoretical calculations propose a mutual disposition of the aromatic fragments at angles of 57.6(4)°, 38.6(1)° and 62.8(4)° in molecule (**1**) as well as 46.7(9)°, 35.0(6)° and 61.5(6)° in (**2**), respectively.

The distribution of the highest occupied (HOMO) and lowest unoccupied (LUMO) molecular orbitals for the ground state is illustrated in Scheme 4. Nearly all of the MOs in the HOMO of (**1**) are substantially localized on the $(CH_3CH_2)_2N$-substituted benzene ring and only small contributions from the other phenyl fragment are observed. In contrast a well-defined distribution in the HOMO and LUMO MOs of the $(CH_3CH_2)_2N$-substituted benzene ring and *N*-ethylpyridinium fragment is observed for (**2**), thus explaining the observed significant bathochromic shift of the λ_{max} value on comparing the electronic spectra of (**1**) and (**2**) (see below).

For a precise investigation of the structural changes associated with the electronic excitation state, the geometries of the studied compounds were optimized for the lowest singlet excited state at the CIS/6-31++G** level of theory to enable a comparison with the data for the ground state optimized at the HF/6-31++G** level. A similar approach has been previously used [24]. The data indicate that the structural shifts are predominantly localized in the conjugated plane of both the benzene and pyridine fragments in the molecules (**1**) and (**2**).

3.3. UV-spectra

The possible redistribution of the electronic density in the newly synthesized compounds as typical push–pull systems depends on the solvent polarity. When the electron transition is connected with intramolecular charge transfer (CT) this leads to a significant difference between the dipole moment in the ground and exited states that determines their significant solvatochromism, or NLO properties in solution. Depending on the type of the solvent the absorption value at λ_{max} of the CT band in *N*,*N*-diethyl-*N*′-[(*Z*)-phenyl(pyridin-4-yl)methylidene]benzene-1,4-diamine decreases (Fig. 4) on going from acetonitrile to acetic anhydride. The observed solvatochromic effect of 98 nm has been explained by both intra- and intermolecular charge transfer. The *N*-ethylpyridinium salt (**2**) is characterized by a 170 nm bathochromic shift of λ_{max} on comparing the electronic spectra of the compounds under identical conditions (Fig. 4). A solvatochromism of 60 nm is observed for (**2**). The theoretically predicted electronic spectra of the compounds

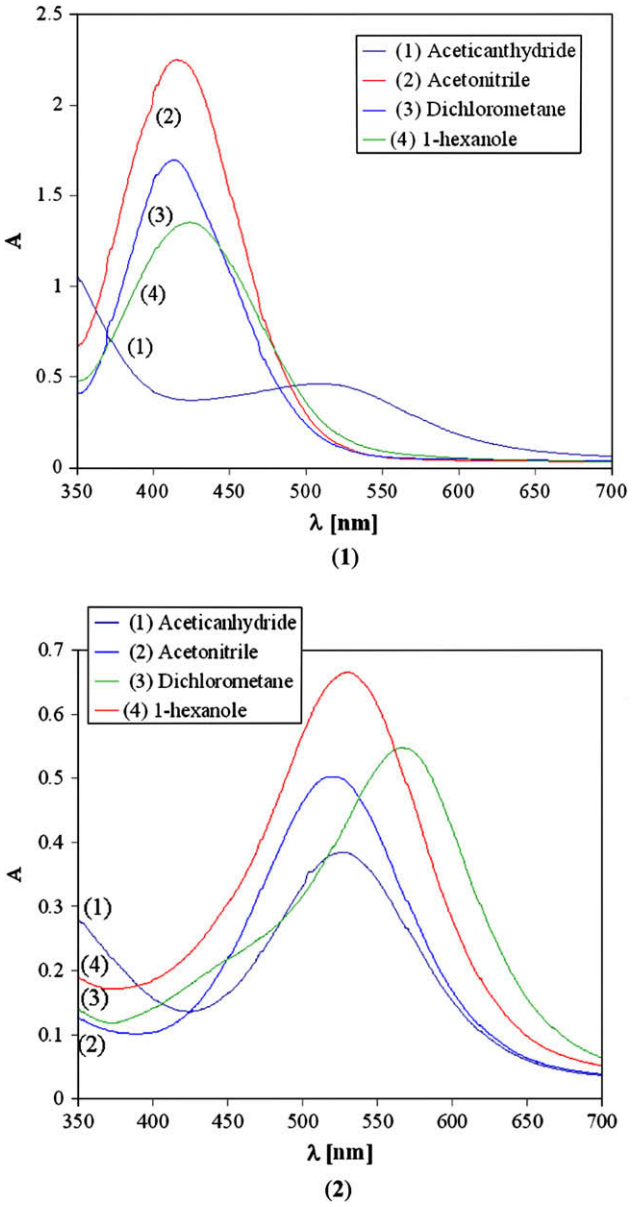

Fig. 4. UV–vis spectra of (**1**) and (**2**) in different solvents at concentration 2.5×10^{-4} mol/l.

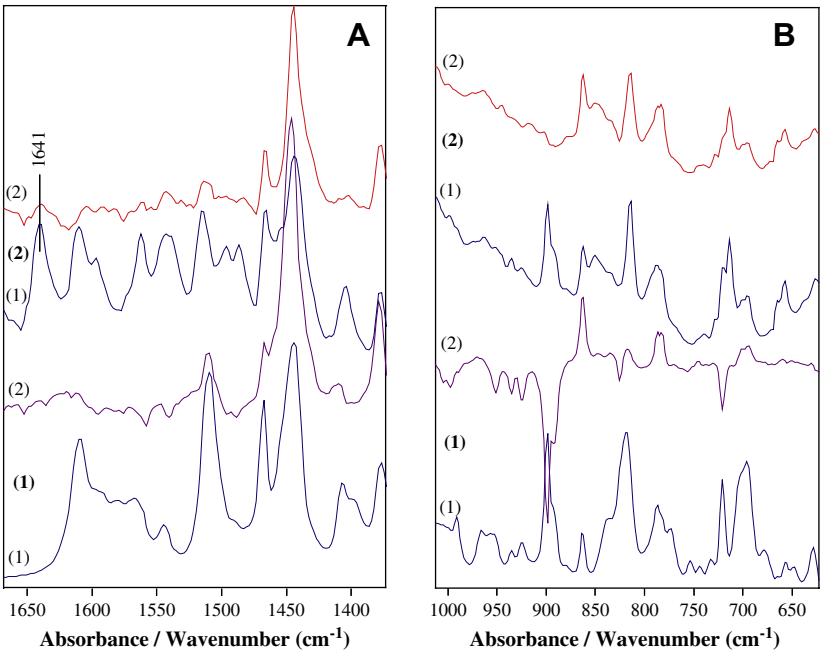

Fig. 5. Non-polarized IR-(1) and reduced IR-LD (2) spectra of compounds (**1**) and (**2**) after elimination of the characteristic i.p. (A) and o.p. (B) IR bands.

show an excellent agreement with the experimental data. In our case, the CIS/6-311++G** method gives a $\Delta\lambda$ difference of 5 nm, while TDDFT calculations generate a better value with a difference of less than 3 nm.

3.4. Conventional and linear polarized IR-spectroscopic data

The effect of *N*-ethylation on the IR-spectroscopic characteristics of (**1**) and (**2**) was elucidated by means of conventional and linear polarized IR-spectroscopy. On comparing both the IR-spectra (Fig. 5A) in the solid state within the region of 1700–1450 cm^{-1} it is apparent that *N*-ethylation does not significantly affect the characteristic in-plane (i.p.) vibrations of both the benzene rings and the pyridinium fragment (bands about 1610 cm^{-1}, 1592 cm^{-1}, 1581 cm^{-1}, 1540 cm^{-1}, 1510 cm^{-1}). As a rule, the second structural fragment is characterized by somewhat higher frequency values of the discussed vibrations, but a difference of less than 2 cm^{-1} is obtained on comparing the data of (**1**) and (**2**). A well-defined band at 1641 cm^{-1} corresponding to the $\nu_{C=N}$ stretching vibration is observed (the theoretical value is 1640 cm^{-1}) in the IR spectrum of (**2**). The relevant maximum is shifted by about 7 cm^{-1} to lower frequency in first compound. The application of the reducing-difference procedure for polarized IR-LD spectra interpretation demonstrates that, on the elimination of the i.p. bands of the pyridine fragment, maxima of the same symmetry class are observed in both cases for the two other aromatic fragments as a result of their mutual cross-orientation in each of the molecules (**1**) and (**2**) (Fig. 5A).

The IR-spectroscopic region within the 900–600 cm^{-1} range is characterized by a series of out-of-plane (o.p.) IR-bands of the three aromatic fragments (Fig. 5B) at about 860 cm^{-1} (o.p. vibration of the pyridine fragment), 820 cm^{-1} (*p*-disubstituted benzene ring) and 721/705 cm^{-1} (monosubstituted benzene ring). The effect of *N*-ethylation leads to a low frequency shifting of the o.p. band of the pyridine fragment of about 9 cm^{-1} (Fig. 5B). Similar to the i.p. bands, the o.p. bands are eliminated at a different dichroic ratio as a result of the cross-orientation of the benzene rings and pyridine fragments in both of the studied compounds.

3.5. ^{1}H and ^{13}C NMR data in solution

The ^{1}H and ^{13}C NMR spectra of the compounds were compared in solution. *N*-Ethylation significantly affects the chemical shifts of the pyridine fragment resonances with the relevant signals being observed at 7.83 ppm and 6.95 ppm, respectively. The resonances of the disubstituted benzene ring at about 7.66 ppm are also shifted by about 0.3 ppm to lower field. These data suggest that the *N*-ethylation leads to a charge distribution that is typical for stybazolium salts [25]. The partial charge redistribution in (**2**) leads to downfield shifts of the signals of the discussed fragments of about 0.5 ppm.

4. Conclusions

The crystal structure and spectroscopic properties of two novel anyles of 4-benzolylpyridine, *i.e. N,N*-diethyl-*N*′-[(*Z*)-phenyl(pyridin-4-yl)methylidene]benzene-1,4-diamine and its *N*-pyridinium iodide have been elucidated by means of linear polarized solid-state IR-spectroscopy, UV-spectroscopy, TGA, DSC, DTA and positive and negative ESI MS. Quantum chemical calculations were used to obtain their electronic structures, vibrational data and electronic spectra. The crystal structure of *N,N*-diethyl-*N*′-[(*Z*)-phenyl(pyridin-4-yl)methylidene]benzene-1,4-diamine represents the first structure of a compound of this type of anyle class to be determined by single crystal X-ray diffraction. Compound (**1**) crystallizes in the triclinic space group and only one short contact between two neighbouring pyridinium fragments is found with a length of 3.16(7)°. A bathochromic shift for λ_{max} of 170 nm is obtained as a result of *N*-anylation and a solvatochromic effect of up to 95 nm is observed for the first compound depending on the solvent type.

Acknowledgements

B.K. wishes to thank the Alexander von Humboldt Foundation for a Fellowship and T.K. the DAAD for a grant within the priority program "Stability Pact South-Eastern Europe" and the Alexander von Humboldt Foundation.

Appendix. Supporting information

Crystallographic data for the structural analysis have been deposited with the Cambridge Crystallographic Data Centre, CCDC 708164. Copies of this information may be obtained from the Director, CCDC, 12 Union Road, Cambridge, CB2 1EZ, UK (fax: +44 1223 336 033; e-mail: deposit@ccdc.cam.ac.uk or http://www.ccdc.cam.ac.uk).

References

[1] Marder SRJ, Perry W, Schaefer WP. Science 1989;245:626.
[2] Marder SR, Perry JW, Tiemann BG, Warsh RE, Schaefer WP. Chem Mater 1990;2:685.
[3] Ashwell GJ, Hargreaves RC, Baldwin CE, Bahra G, Brown CR. Nature 1992;357:6377.
[4] Lupo D, Prass W, Scheunemann U, Laschewsky A, Ringsdorf R, Ledoux I. J Opt Soc Am B 1988;5:300.
[5] Kolev TM, Yancheva DY, Stoyanov SI. Adv Func Mater 2004;14:799.
[6] Kolev T, Wortmann R, Spiteller M, Sheldrick WS, Heller M. Acta Crystallogr 2004;E60:o1374.
[7] Kolev T, Wortmann R, Spiteller M, Sheldrick W, Mayer-Figge H. Acta Crystallogr 2005;E61:o1090.
[8] Kolev T, Stamboliyska B, Yancheva D. Chem Phys 2006;324:489.
[9] Sheldrick GM. SHELXTL, Release 5.03 for Siemens R3 crystallographic research system. Madison, USA: Siemens Analytical X-Ray Instruments, Inc.; 1995.
[10] Sheldrick GM. SHELXS97 and SHELXL97. Germany: University of Goettingen; 1997.
[11] Ivanova BB, Arnaudov MG, Bontchev PR. Spectrochim Acta Part A 2004;60:855.
[12] Ivanova BB, Tsalev DL, Arnaudov MG. Talanta 2006;69:822.
[13] Ivanova B, Simeonov V, Arnaudov M, Tsalev D. Spectrochim Acta 2007;67A:66.
[14] Koleva BB, Kolev TM, Simeonov V, Spassov T, Spiteller M. J Inclus Prenom 2008;. doi:10.1007/s10847-008-9425-5.
[15] Ivanova BB. Spectrochim Acta 2006;64A:931.
[16] Ivanova BB, Kolev T, Zareva S. Biopolymers 2006;82:587.
[17] Kolev Ts. Biopolymers 2006;83:39.
[18] Jordanov B, Schrader B. J Mol Struct 1995;347:389.
[19] Jordanov B, Nentchovska R, Schrader B. J Mol Struct 1993;297:2922.
[20] Michl J, Thulstrup EW. Spectroscopy with polarized light. Solute alignment by photoselection, in liquid crystals, polymers, and membranes. N.Y.: VCH Publishers; 1986.
[21] Thulstrup EW, Eggers JH. Chem Phys Lett 1996;1:690.
[22] Frisch MJ, Trucks GW, Schlegel HB, Scuseria GE, Robb MA, Cheeseman JR, et al. Gaussian 98. Pittsburgh, PA: Gaussian, Inc.; 1998.
[23] Zhurko GA, Zhurko DA. ChemCraft: tool for treatment of chemical data, Lite version build 08 (freeware); 2005.
[24] Ju X, Ju H, Zhao H, Tao X, Bian W, Jiang M. J Chem Phys 2006;124:174711.
[25] Kolev Ts, Koleva BB, Spiteller M, Mayer-Figge H, Sheldrick WS. Dyes Pigments 2008;79:7.